Mid-infrared tunable optical polarization converter composed of asymmetric graphene nanocrosses

Hua Cheng,[1] Shuqi Chen,[1,*] Ping Yu,[1] Jianxiong Li,[1] Li Deng,[1] and Jianguo Tian[1,2]

[1]*The Key Laboratory of Weak Light Nonlinear Photonics, Ministry of Education, School of Physics and TEDA Applied Physics School, Nankai University, Tianjin 300071, China*

[2]*e-mail: jjtian@nankai.edu.cn*

**Corresponding author: schen@nankai.edu.cn*

Received February 6, 2013; revised March 20, 2013; accepted April 3, 2013; posted April 8, 2013 (Doc. ID 185011); published April 30, 2013

We present a mid-IR highly tunable optical polarization converter composed of asymmetric graphene nanocrosses. It can convert linearly polarized light to circularly and elliptically polarized light or exhibit a giant optical activity at different wavelengths. The transmitted wavelength and polarization states can also be dynamically tuned by varying the Fermi energy of graphene, without reoptimizing and refabricating the nanostructures. This offers a further step in developing a controllable polarization converter.

OCIS codes: (160.3918) Metamaterials; (240.6680) Surface plasmons; (260.5430) Polarization.
http://dx.doi.org/10.1364/OL.38.001567

Manipulating the state of optical polarization is of central interest in efficiently controlling light, as required in many applications. Optical activity can be widely used in many areas, such as optics, analytical chemistry, crystallography, and molecular biology. The ability to create and detect circular or elliptical polarization is of great interest in advanced optical signaling and biological sensors because of its inherent robustness to scattering and diffraction [1]. The conventional methods used to manipulate the polarization of light are based on effects, such as Faraday, Kerr, and birefringence effects. These methods typically require a system much thicker than wavelength, which is inconvenient for low-frequency applications. Recently, researchers have found that metamaterials and surface plasmon polariton structures can be used to control the polarization state of light at the nanoscale. These structures include crossed resonant plasmonic nanostructures [2], elliptical patch nanoantennas [3] and three-dimensional chiral metamaterials [4,5]. All of these structures exploit the strong field localization and enhancement due to localized light interaction with surface plasmons or spoof surface plasmon modes. Moreover, the polarization state of light has to be tuned by accurately fabricating different nanostructures, which is an inherent drawback.

Graphene is a single two-dimensional plane of carbon atoms arranged in a honeycomb lattice and has been demonstrated both theoretically [6] and experimentally [7] to excite and propagate surface plasmons. It has attracted increasing attention because of its novel photonic and optoelectronic applications [8], such as complete optical absorption [9], plasmon waveguiding [10], and photodetectors [11]. Compared to traditional metal plasmonics, the most important advantage with graphene is the capability of dynamically tuning the conductivity through chemical or electrostatic gatings [12]. In addition, graphene has a tighter confinement of the surface plasmons to graphene layers, which supports a stronger electromagnetic field platform for light–matter interactions [6,10]. Therefore, designing a dynamically tunable optical polarization converter based on graphene remains an ongoing interest in the development of novel, compact elements to control the polarization states of both reflected and transmitted light.

In this Letter, we present a highly tunable optical polarization converter composed of asymmetric graphene nanocrosses in the mid-IR region. We demonstrate that the graphene nanocrosses can convert linearly polarized light to circularly and elliptically polarized light or exhibit a giant optical activity at different wavelengths. Moreover, both the wavelength and polarization states can be dynamically tuned by varying the Fermi energy of graphene, without reoptimizing and refabricating the nanostructures, which offers possible application as a controllable polarization converter.

The designed optical polarization converter based on graphene nanocrosses is shown in Fig. 1. The optimized graphene structure was achieved using COMSOL Multiphysics [13]. A single unit cell with periodic boundary conditions in all x–z and y–z planes is considered, and perfectly matched layers are defined in the z direction to terminate the upper and lower surfaces. The refractive index of the substrate is considered to be 1.5. The conductivity of graphene (see Eq. (1) in [6]) was computed within the local random phase approximation (local-RPA) limit with an intrinsic relaxation time $\tau = \mu E_F/ev_F^2$, where $v_F \approx c/300$ is the Fermi velocity and $\mu = 10000$ cm^2/Vs is the measured DC mobility [14]. Then, the dielectric constant of graphene can be obtained by $\varepsilon = 1 + i\sigma/(\varepsilon_0\omega\delta)$, where δ is the thickness of graphene.

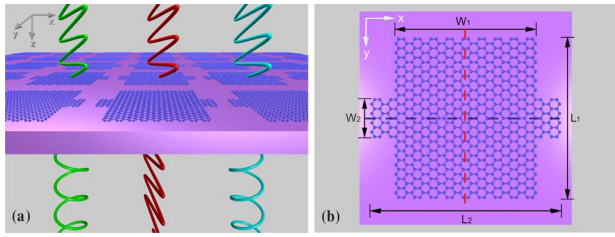

Fig. 1. (a) Schematic model of asymmetric graphene nanocrosses on a substrate and (b) unit cell structure of our design: $L_1 = 70$ nm, $W_1 = 63$ nm, $L_2 = 80$ nm, $W_2 = 16$ nm, and the periodicity is 90 nm. Red (vertical) and blue (horizontal) dashed lines indicate the cutting positions.

Let us consider the illumination of a normally incident plane wave, propagating along the $+z$ direction. The transmission coefficients of x- or y-polarized transmitted waves are defined as $T_{ij} = |E_j^{\mathrm{Trans}}/E_i^{\mathrm{Inc}}|(i, j = x, y)$, where E_i^{Inc} $(i = x, y)$ is the electric field of the x- or y-polarized incident wave and E_j^{Trans} $(j = x, y)$ is the x or y component of the electric field of the transmitted waves, respectively. Meanwhile, the phase of x- or y-polarized transmitted waves is defined as $\Phi_{ij} = \arg(E_j^{\mathrm{Trans}}/E_i^{\mathrm{Inc}})$ $(i,j = x, y)$;. The transmission coefficients and phase difference $\Delta\Phi = \Phi_{xx} - \Phi_{yy}$ are shown in Fig. 2. The optimized asymmetric graphene nanocrosses show two distinct resonances illuminated by orthogonal linear polarizations aligned along the x and y directions. The strong resonances demonstrate very efficient excitation of surface plasmons in graphene. Surface plasmon excitations in asymmetric graphene nanocrosses correspond to collective oscillations of electrons across each length of nanobars (L_1, L_2), where plasmon frequency scales with different bar length. The z components of an electric near field at the resonant wavelengths in the x–z and y–z planes along the red and blue dashed lines in Fig. 1(b) are shown in the insets of Fig. 2(a). The origin of the resonance can be interpreted as the dipolar modes coupled to propagating light, which has a strong field concentration near nanocross edges and a strong interaction with the neighboring structures [10]. When the phase difference is exactly 90° at a wavelength of 7.92 μm with $T_{xx} = T_{yy}$, an ultrathin quarter-wave plate can be realized. When the phase difference is 0° at 7.85 or 7.99 μm, an optical activity can be achieved. At wavelengths other than these three specific wavelengths, the phase difference will satisfy $\Delta\Phi \neq n\pi/2$ $(n = 0, 1, 2, \ldots)$, resulting in elliptically polarized transmissions.

To verify optical activity at 7.85 and 7.99 μm and the achievement of a quarter wave plate at 7.92 μm, we calculated the amplitude ratio and phase difference between the x and y components of the transmission coefficient versus the incident polarization angle, as shown in Figs. 3(a)–3(c). Linearly polarized light with normal incidence to the surface of asymmetric graphene nanocrosses was considered. The polarization angle is defined as the angle between the polarization direction and the $+x$ direction. Results show that the phase difference is always 0 at 7.85 and 7.99 μm, indicating that an

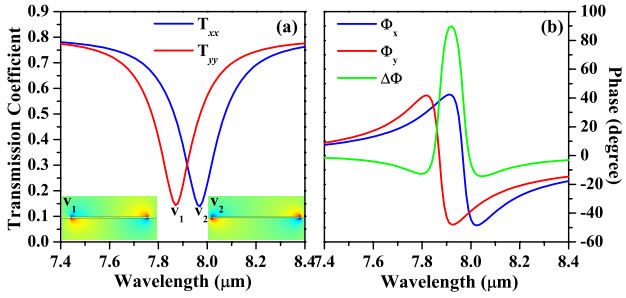

Fig. 2. (a) Calculated transmission coefficients and (b) phase difference excited by linearly polarized light. The Fermi energy is 0.75 eV. Insets: z components of the electric near-field in the x–z and y–z planes.

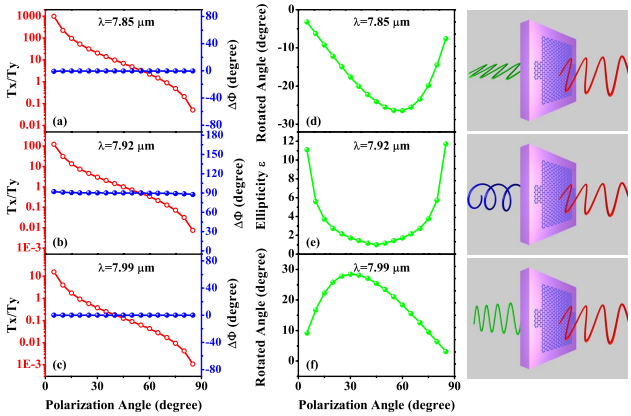

Fig. 3. (a)–(c) Amplitude ratio and phase difference versus the incident polarization angle at different wavelengths and (d)–(f) the rotated polarization angle and ellipticity versus the incident polarization angle at different wavelengths. The Fermi energy is 0.75 eV. The right images indicate that the graphene nanocrosses can exhibit a giant optical activity or conversation at different wavelengths.

optical activity is obtained. The corresponding rotated polarization angles are shown in Figs. 3(d) and 3(f), which varied with the incident polarization angles. The maximum rotated angle is approximately 28°, as the incident polarization angles are 60° and 30° for 7.85 and 7.99 μm, respectively. When the incident polarization angle was 45°, circularly polarized transmission light was realized, since $\Delta\Phi = 90^{\circ}$ and $T_x/T_y = 1$ were maintained. For incident polarization angles other than 45°, elliptically polarized transmission light was realized. Likewise, by using the elliptic equation [15],

$$\frac{E_x^2}{|E_x|^2} + \frac{E_y^2}{|E_y|^2} - \frac{E_x E_y}{|E_x||E_y|}\cos(\Delta\Phi) = \sin^2(\Delta\Phi), \qquad (1)$$

we can obtain the transmitted polarization state for any incident polarization angle. We calculated the ellipticity ε (the major-to-minor-axis ratio) of the elliptically polarized transmission light for 7.92 μm, as shown in Fig. 3(e). The ellipticity decreases first and then increases with the incident polarization angle, reaching a minimum value of 1 for an incident polarization angle of 45°. As the ellipticity ε decreases toward 1, the elliptically polarized transmission light gradually approaches circularly polarized transmission light.

In order to demonstrate the polarization conversion tunability for the proposed asymmetric graphene nanocross, we graphed the amplitude ratio and phase difference between the x and y components of the transmission coefficient as a function of Fermi energy and wavelength, as shown in Fig. 4. As the Fermi energy increased, both the maximum amplitude ratio and the phase difference increased and blue-shifted. This behavior can be interpreted by the resonance condition. The wave vectors of surface plasmons along the x and y directions of the nanocrosses satisfy $k_{(\mathrm{spp})i,j} \propto 1/L_{i,j}$ $(i, j = x, y)$ [10], where $L_{i,j}$ $(i, j = x, y)$ represents the bar length of the nanocrosses along the x or y directions. In addition, the surface plasmons in graphene with the

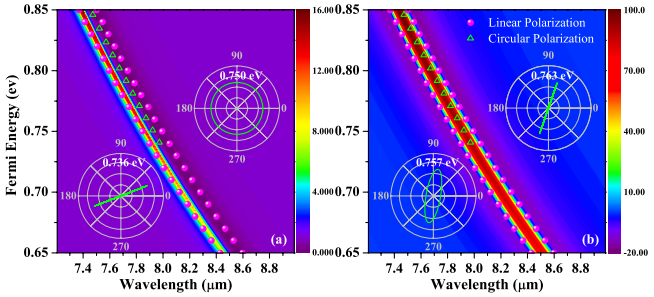

Fig. 4. (a) Calculated amplitude ratio and (b) phase difference as a function of the Fermi energy and wavelength. Inset images show the transmitted polarization state for different Fermi energies at a wavelength of 7.92 μm. The incident light is linearly polarized with a polarization angle of 45°.

considered frequency range approximately satisfy $k_{\mathrm{spp}} = \hbar\omega^2/(2\alpha_0 E_F c)$ [10], where $\alpha_0 = e^2/(\hbar c)$ is the fine structure constant. Thus, the surface plasmon wavelengths can be written as $\lambda_{(\mathrm{spp})i,j} \propto \sqrt{2\pi^2\hbar c L_{i,j}/(\alpha_0 E_F)} \propto \sqrt{L_{i,j}/E_F}$. Hence, the resonant wavelengths can be tuned by changing the Fermi energy while fixing the geometrical parameters, indicating that graphene polarization converters are more active than metallic polarization converters. The phase difference of solid spheres shown in Fig. 4 is 0°, where a linearly polarized transmission light can be achieved. For a fixed Fermi energy, optical activity can be achieved at two wavelengths. Meanwhile, the amplitude ratio and phase difference of hollow triangles in Fig. 4 are 1 and 90°, respectively, where a circularly polarized transmission light can be obtained. However, the above conditions cannot be simultaneously satisfied when the Fermi energy is less than 0.74 eV.

In conclusion, we have proposed a highly tunable optical polarization converter in the mid-IR region based on asymmetric graphene nanocrosses. Elliptically, circularly, and linearly polarized light transmission can be obtained at different wavelengths for a fixed Fermi energy. Moreover, both of the transmitted wavelength and polarization states can be dynamically tuned by only varying the Fermi energy, without reoptimizing and refabricating the nanostructures. This makes graphene polarization converters more useful than metallic polarization converters. As it works in the transmission regime, transparent conductors should be employed as gate material in the practical realization. With geometrical scalability and Fermi energy variability, this concept can also be realized at the terahertz region. We believe this polarization modulation method enables us to modulate electromagnetic wave polarizations. This is potentially useful in applications, such as vibrational circular dichroism spectroscopy, ellipsometry, and integration of other optical devices for polarization manipulation, detection, and sensing at the nanoscale.

This work was supported by the 973 Program (2012CB921900), the CNKBRSF (2011CB922003), the NSFC (61008002), the SRFDP (20100031120005 and 20120031120032), and the 111 Project (B07013).

References

1. Y. Huang, Y. Zhou, and S. Wu, Opt. Express **15**, 6414 (2007).
2. A. Pors, M. G. Nielsen, G. D. Valle, M. Willatzen, O. Albrektsen, and S. I. Bozhevolnyi, Opt. Lett. **36**, 1626 (2011).
3. F. Wang, A. Chakrabarty, F. Minkowski, K. Sun, and Q. Wei, Appl. Phys. Lett. **101**, 023101 (2012).
4. C. Helgert, E. Pshenay-Severin, M. Falkner, C. Menzel, C. Rockstuhl, E. Kley, A. Tünnermann, F. Lederer, and T. Pertsch, Nano Lett. **11**, 4400 (2011).
5. M. Mutlu, A. E. Akosman, A. E. Serebryannikov, and E. Ozbay, Opt. Lett. **36**, 1653 (2011).
6. F. H. L. Koppens, D. E. Chang, and F. J. G. de Abajo, Nano Lett. **11**, 3370 (2011).
7. L. Ju, B. Geng, J. Horng, C. Girit, M. Martin, Z. Hao, H. A. Bechtel, X. Liang, A. Zettl, Y. R. Shen, and F. Wang, Nat. Nanotechnol. **6**, 630 (2011).
8. F. Bonaccorso, Z. Sun, T. Hasan, and A. C. Ferrari, Nat. Photonics **4**, 611 (2010).
9. S. Thongrattanasiri, F. H. L. Koppens, and F. J. G. de Abajo, Phys. Rev. Lett. **108**, 047401 (2012).
10. J. Christensen, A. Manjavacas, S. Thongrattanasiri, F. H. H. Koppens, and F. J. G. de Abajo, ACS Nano **6**, 431 (2012).
11. F. N. Xia, T. Mueller, Y. M. Lin, A. Valdes-Garcia, and P. Avouris, Nat. Nanotechnol. **4**, 839 (2009).
12. K. F. Mark, M. Y. Sfeir, Y. Wu, C. H. Lui, J. A. Misewich, and T. F. Heinz, Phys. Rev. Lett. **101**, 196405 (2008).
13. COMSOL Multiphysics User's Guide., Version 3.5 (Comsol AB, Brulington, Massachusetts, 2008).
14. K. S. Novoselov, A. K. Geim, S. V. Morozov, D. Jiang, Y. Zhang, S. V. Dubonos, I. V. Grigorieva, and A. A. Firsov, Science **306**, 666 (2004).
15. J. D. Jackson, *Classical Electrodynamics* (Wiley, 1999).